Conf-930676--14

LA-UR 93-2468

Los Alamos National Laboratory is operated by the University of California for the United States Department of Energy under contract W-7405-ENG-36.

TITLE: LIQUID SOUND SPEEDS AT PRESSURE FROM THE OPTICAL ANALYZER TECHNIQUE

AUTHOR(S): JOSEPH N. FRITZ, M-6
CHARLES E. MORRIS, M-6
ROBERT S. HIXSON, M-6
ROBERT G. MCQUEEN, M-6

SUBMITTED TO XIV INTERNATIONAL CONFERENCE ON HIGH PRESSURE SCIENCE AND TECHNOLOGY AND 1993 TECHNICAL MEETING OF THE TOPICAL GROUP ON SHOCK COMPRESSION OF CONDENSED MATTER
JUNE 28-JULY 2, 1993
COLORADO SPRINGS, CO

Los Alamos National Laboratory
Los Alamos, New Mexico 87545

LIQUID SOUND SPEEDS AT PRESSURE FROM THE OPTICAL ANALYZER TECHNIQUE*

J. N. Fritz, C. E. Morris, R. S. Hixson,and R. G. McQueen
M6, MS C970
Los Alamos National Laboratory
Los Alamos, New Mexico 87545 USA

The optical analyzer technique has proved to be a useful means of obtaining wave velocities at high pressures. Stepped wedges of the investigated material emit shock, and later, rarefaction waves into a transparent analyzer covering the material. The time interval between shock and rarefaction plotted versus wedge thickness gives a linear plot whose intercept fixes the target/driver thickness ratio for exact wave overtake, and thus gives a relation between the shock velocity and overtaking wave velocity at pressure. The *slope* of this line is intimately related to the wave velocity at pressure of the *analyzer* in front of the wedge. This aspect of the technique has not yet been exploited. We present the appropriate analysis, some data on bromoform (one of the analyzers used), and discuss some possible applications of this technique.

INTRODUCTION

The optical analyzer technique[1] has been used to measure release velocities in a variety of metals. Sound-speed accuracies of the order 1% allow determination of derivatives on the equation-of-state surface to the same level of accuracy as Hugoniot states. Several high-pressure phase transitions have been detected in metals that were not apparent from the Hugoniot data. We will show how the optical analyzer technique can be used to measure sound speeds in liquids. Accurate bulk moduli can be determined for validation of theoretical models, in addition to the possible detection of phase transitions such as shock-induced dissociation and ionization. In the conventional application of the optical analyzer technique, the overtake time in the liquid analyzer (usually bromoform) decreases linearly with increasing target thickness. From the intercept of this overtake curve on the target thickness axis the rarefaction velocity in the target can be determined. The information that hasn't been exploited with this technique is the slope of the overtake curve. We will demonstrate that this slope is intimately related to the sound velocity in the liquid analyzer. Several shots have been analyzed using stainless-steel targets to measure sound speeds in bromoform. These efforts were quite successful. We believe this technique can also be used on liquids at cryogenic temperatures. Because the liquid needs to radiate like a black body to simply correlate radiation records with wave arrival, high-pressure experiments are particularly suited to this technique.

WAVE RELATIONS

Our results will be obtained from an analysis of lead characteristics propagating into constant states. Fig. 1, in the time-Lagrangian coordinate (t–y) plane shows the waves of interest. The dotted lines are applicable for impacts between the stainless steel driver and target that produce pressures less than those that result in melting on the Hugoniot ($P < 227\,\mathrm{GPa}$). We analyze the fluid case (the solid lines) first.

Our direct observable $\Delta t = t_{96}$ (we use $x_{ij} \equiv x_i - x_j$) is a function of the target thickness $T = y_3 = y_6 = y_8$. Several target thicknesses from the step wedges in an experiment result in the $\Delta t(T)$ shown in Fig. 2. From such a plot we get the intercept thickness T_0 and a velocity from the

*This work supported by the US Department of Energy.

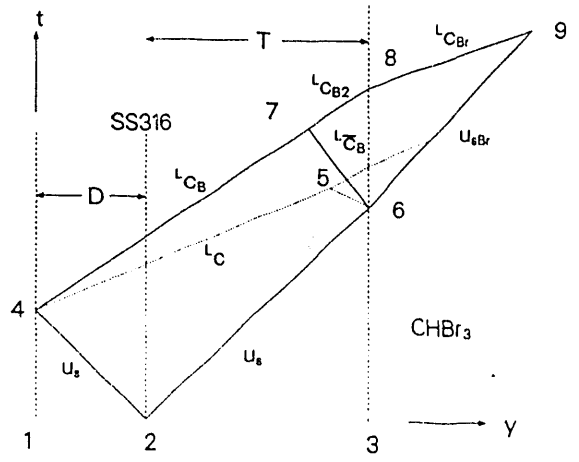

Figure 1. The t–y diagram for the overtake experiment. A driver plate of thickness D moving at a velocity u_D impacts the target, thickness T, at 2. For a symmetric impact shocks with the same velocity u_s propagate through driver and target. A release is generated at the back surface of the driver at 4. If the shock is strong enough to melt the driver and target the lead characteristic is the beginning of the bulk rarefaction fan; otherwise it is an elastic wave. In front of the target we have a reservoir of bromoform. The shock state in the target interacts with the bromoform at 6. A release goes back into the target and a shock goes forward into the bromoform. The overtaking wave goes through various interactions and catches up with the shock. Radiation from the shock front in bromoform, along the path 6 → 9 (and farther) is observed, and enables the identification of the times t_6 and t_9.

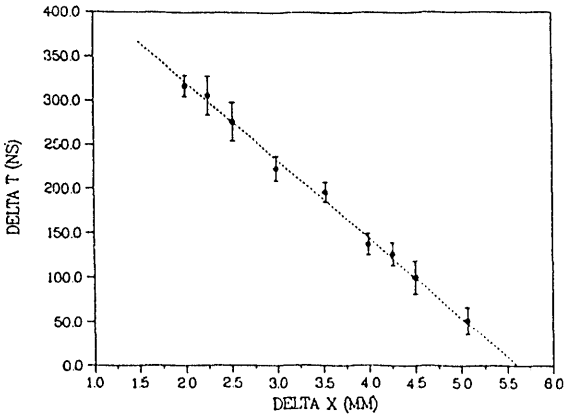

Figure 2. $\Delta t(T)$. The plot shows the 9 overtake levels obtained in an explosively-driven experiment. An intercept of T_0 =5.6 mm and a v^* =11.25 km/s was obtained from this plot.

slope $1/v^* = -d(\Delta t)/dT$. We have $y_{98} = {}^{l}c_{Br}t_{98}$ and $y_{96} = u_{sBr}t_{96}$. Elimination of t_9 then implies $(y_9 - T)(1/u_{sBr} - 1/{}^{l}c_{Br}) = t_{86}$ and

$$t_{96} = t_{86}/(1 - u_{sBr}/{}^{l}c_{Br}) \qquad (1)$$

Our information on the bromoform sound speed is contained in the second factor. We will be measuring the ratio of the shock and Lagrangian sound velocities. We now need to evaluate dt_{86}/dT. Such derivations follow the above pattern; finding the intersections of straight characteristics. *If* the rarefaction from interaction 6 did not change the slopes of the lead characteristics we would have

$$t_{86} = D(\frac{1}{u_s} + \frac{1}{{}^{l}c_B}) - T(\frac{1}{u_s} - \frac{1}{{}^{l}c_B}) \qquad (2)$$

This assumption *is valid* for locating the intercept. When this time interval vanishes, we have $R \equiv T_0/D$, $R = (1 + u_s/{}^{l}c_B)/(1 - u_s/{}^{l}c_B)$, $u_s/{}^{l}c_B = (R-1)/(R+1)$, $1 - u_s/{}^{l}c_B = 2/(R+1)$. From eq. (2) we obtain $dt_{86}/dT = -2f/(u_s(R+1))$. We have to put in an additional factor f, a function of the intermediate velocities, to account for the important changes caused by the rarefaction fan emanating from interaction 6. We then have

$$1 - \frac{u_{sBr}}{{}^{l}c_{Br}} = f\frac{2v^*}{(R+1)u_s} \qquad (3)$$

A full solution of the t–y diagram for the fluid case yields an equation like (2) except for an additional factor f on the right hand side given by

$$f_{\text{fluid}} = \frac{1 + {}^{l}\bar{c}_B/{}^{l}c_{B2}}{1 + {}^{l}\bar{c}_B/{}^{l}c_B} \qquad (4)$$

The actual t–y diagram at interaction 7 is the lead characteristic from 4 interacting with a rarefaction fan from 6. The lead characteristic of the fan has the velocity ${}^{l}c_B$, and tail characteristic has the bulk velocity associated with the state produced at interaction 6, ${}^{l}c_{B2}$. The effect of a curved path through the extended interaction 7 is accurately represented by using a single ray carrying the rarefaction which has the velocity ${}^{l}\bar{c}_B$, a velocity corresponding to the chord slope obtained from the

two state points on the isentrope representation in the P–u_p plane. When we use eq. (4) in (3) we replace ${}^Lc_B$ everywhere by its experimental equivalent $u_s(R+1)/(R-1)$. In order to evaluate the remaining terms in $f_{\rm fluid}$, ${}^L\bar{c}_B$ and ${}^Lc_{B2}$, we assume the usual $u_s(u_p)$ Hugoniot, a Mie-Grüneisen $E(P,V)$, and a constant $\rho\gamma$.

For the elastic-wave solution we slide interactions 7,8,9 down to the dotted line. The lead characteristics from 4 → 5 and 6 → 5 travel with velocity ${}^Lc = u_s(R+1)/(R-1)$, the experimental longitudinal velocity given by the measured intercept T_0. The waves from 5 → 7 and 7 → 8 carry a release in material that has already been relieved elastically, so we assume that these waves travel with velocities ${}^Lc_B$ and ${}^Lc_{B2}$, i.e., velocities appropriate to the bulk properties of the material. We are assuming that the initial elastic release drops the steel to its lower yield surface, and that the amplitude of this elastic release does not greatly change the bulk state (in particular its effect on calculating the f-factor), and that further wave propagation in the steel is at the bulk velocities. When we solve the t–y diagram for the elastic case we again get an equation similar to (2) with an f given by

$$f_{\rm elastic} = f_{\rm fluid}\frac{1+{}^Lc/{}^Lc_B}{2} \qquad (5)$$

In this case we will replace ${}^Lc$ by its experimental equivalent $u_s(R+1)/(R-1)$ and use the EOS information for 316 stainless steel[2] and $CHBr_3$[3] to evaluate the intermediate velocities. The EOS's used for these two materials are: SS316($\rho_0 = 7.96$, $u_s = 4.464 + 1.544u_p$, $\rho\gamma = 17.27$) and $CHBr_3$($\rho_0 = 2.87$, $u_s = 1.50 + 1.38u_p$). Units are g/cm^3 and km/s. The SS316 EOS should be regarded as tentative, particularly if it is used above the melting transition.

RESULTS

Experimental values for v^*, R, and u_s are used in eq. 3 to obtain ${}^Lc_{\rm Br}$. The resulting sound speed at pressure in bromoform, $c_{\rm Br}(\rho) = \rho_0{}^Lc_{\rm Br}/\rho$, is shown in Fig. 3.

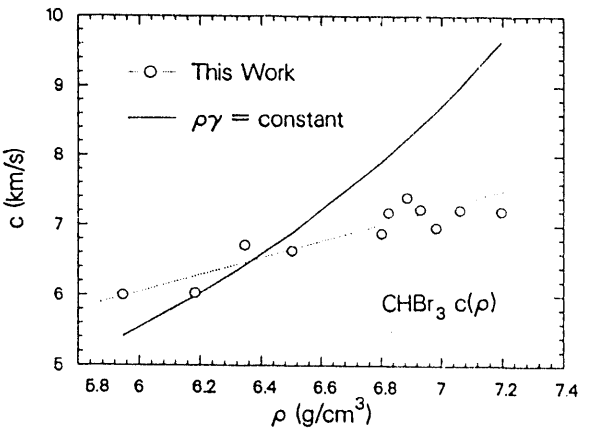

Figure 3. Bromoform Sound Speed vs Density.

When we measure sound speed in a liquid along the Hugoniot we also get the Grüneisen function. If $B = -VdP/dV$ for a curve, a convenient expression for γ is:

$$\frac{\gamma}{2V}(V_0 - V) = \frac{B_h - B_s}{B_h - B_{ch}} \qquad (6)$$

where the subscripts refer to the Hugoniot, isentrope, and Rayleigh ray. (An ambiguity exists for the chord slope; in writing the above form we have chosen $B_{ch} = V(P-P_0)(V_0-V)$.) If the Hugoniot can be represented as a linear $u_s(u_p)$ a convenient computational form is:

$$\gamma\left(\frac{\rho}{\rho_0} - 1\right) = \frac{(c_0 + 2su_p) - c_0({}^Lc/u_s)^2}{su_p} \qquad (7)$$

The results for γ are shown in Fig. 4. The first and third data points are suspect. They lead to γ-values that are rather low. The linear fit to $c(\rho)$ shown is: $-1.2 + 1.21\rho$, and the scatter is such that $c(\rho_0) = 1.5$ readily fits within the uncertainty. Lowering the sound speed of the first

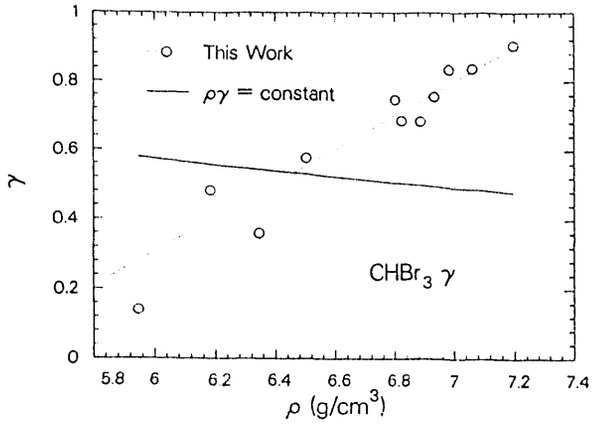

Figure 4. Bromoform $\gamma_h(\rho)$.

and third points (and increasing γ) is a move in the direction of a good linear $c(\rho)$ that would extend down to ρ_0.

The $\rho\gamma$ constant assumption is an approximation that is adequate for modest compression. It was never intended for the compressions achieved here. It may describe the initial drop from the thermodynamic $\gamma_0 = 1.2$. Even discounting the two lower values of γ, it seems to have dropped to 0.5, a low value perhaps induced by disassociation and the opening of miscellaneous energy sinks; and then has risen toward (and perhaps past) the value 2/3, a γ characteristic of a hot electron gas.

Exceeding the value 2/3 may be a consequence of extrapolating the linear $u_s(u_p)$ fit of SS316 past its melting point. Some preliminary data exist that indicate this linear fit overestimates u_s for a given u_p for shock strengths beyond the melting point. Use of such a lowered Hugoniot could readily drop the γ-points from the melted regime (the last five points) toward 2/3 and lead to a constant γ in this region.

DISCUSSION

This technique has the great advantage of not needing any structure in the liquid reservoir. Precision resides in the driver/target assembly. As our knowledge of driver/target behavior improves, we will be better able to estimate the f-factors required to implement this technique. For these experiments the f values have been around 1.25. It is already a method that shows great promise for making these measurements in any transparent material that becomes sufficiently ionized in a shock.

We have not yet done an error analysis for this technique. Space available here precludes this. Because bromoform has been used as an analyzer on many different materials there are about a hundred or so shots waiting in the wings to be analyzed. Analysis of this wealth of data and the necessary error analysis is in progress. The bromoform high-pressure sound speed and its $\gamma(\rho)$ may turn out to be one of our most accurate high-pressure data curves; it will certainly be one with a high density of data points.

We have used this analysis for points where the driver/target is in the elastic regime (the lower six points) and where it has melted (the upper five). The bromoform data is smooth between these two data sets, even though the driver/target system exhibits a relative large discontinuity from one to the other. This is as it should be and lends some confidence to our use of the f-factors in the two different regimes.

REFERENCES

1. R. G. McQueen, J. W. Hopson, and J. N. Fritz. Optical technique for determing rarefaction wave velocities at very high pressures. *Rev. Scient. Instr.*, 53(2):245–250, February 1981.
2. R. S. Hixson, R. G. McQueen, and J. N. Fritz. The shock hugoniot of SS316 and sound velocity measurements. These proceedings.
3. R. G. McQueen and D. G. Isaak. Bromoform ($CHBr_3$) – a very high-pressure shock-wave analyzer. In S. C. Schmidt, J. N. Johnson, and L. W. Davison, editors, *Shock Waves in Condensed Matter – 1989*, pages 125–128. North Holland, Amsterdam, 1990.

END

DATE
FILMED
10/7/93